Electronic Supplementary Material (ESI) for Chemical Science
This journal is © The Royal Society of Chemistry 2013

Supporting Information

A Light-induced Reversible Phase Separation and its Coupling to a Dynamic Library of Imines

Ghislaine Vantomme, Nema Hafezi, and Jean-Marie Lehn*

Experimental part:

Irradiations were carried out with a Müller Elektronik Optik Light Source Model LAX 1000 / SVX 1000 with a xenon short arc lamp XBO 1000 W / HS OFR from Osram. The experiments were performed in a glass thermostated bath at 25°C.

Synthesis of deuterated (α-*d*,6-*d*)**1-E**:

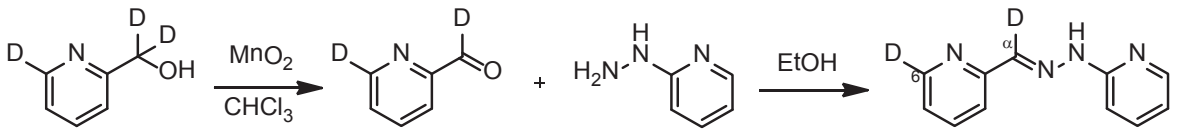

(α-*d*,6-*d*)**1-E** 62%

6-deuterio-2-pyridinecarboxaldehyde-α-d-2-pyridylhydrazone ((α-*d*,6-*d*)**1-E**) - A solution of 2-pyridine-*6-d*-methan-α,α-d_2-ol-*d* [1] (1.26 g, 11.1 mmol) in 50 mL of $CHCl_3$ was treated with MnO_2 (4.00 g, 46.0 mmol) and heated to reflux for 14 hours under nitrogen. The suspension was cooled to room temperature and filtered through a pad of celite. The filter cake was washed with $CHCl_3$, and the combined filtrates were evaporated, giving the crude 6-deuterio-2-pyridinecarboxaldehyde-alpha-d, which was immediately carried over to the next step.

The crude aldehyde was dissolved in 50 mL of absolute ethanol and treated with 2-hydrazinopyridine (1.21 g, 11.1 mmol). The mixture was heated to reflux under nitrogen for 12 hours and evaporated to dryness, giving a tan solid. Recrystallization from $CHCl_3$/Et_2O gave **1-E** as colorless needles (1.38 g, 6.89 mmol, 62%, 95% *D*).

^{1}H NMR ($CDCl_3$): 8.20 (d, *J* = *4.49*, 1H), 7.99 (d, *J* = *8.03*, 1H), 7.69 (t, *J* = *7.63*, 1H), 7.63 (t, *J* = *7.84*, 1H), 7.42 (d, *J* = *8.49*, 1H), 7.19 (d, *J* = *7.20*, 1H), 6.82 (dd, *J* = *7.40*, *J* = *5.51*, 1H); ^{13}C NMR ($CDCl_3$): 156.7, 154.3, 149.1 (t, J = 26.9), 147.4, 139.3 (t, J = 24.3), 138.4, 136.4, 122.9, 119.9, 116.4, 107.9. MS calculated for $[C_{11}H_8D_2N_4+H]^+$ 201.1104, found 201.1109. Traces of $[C_{11}H_9D_1N_4+H]^+$ 200.1041, found 200.1039 and $[C_{11}H_{10}N_4+H]^+$ 199.0978, found 199.0981.

This journal is © The Royal Society of Chemistry 2013

Figures:

Calcium binding by hydrazone 1.

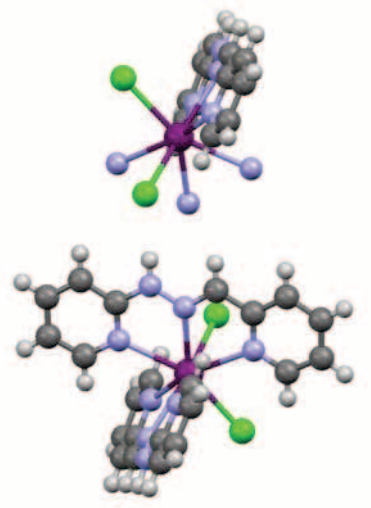

Fig. 1 Solid state molecular structure of the [(**1-E**)$_2$,**Ca**]**Cl**$_2$ complex showing that each chloride anion is hydrogen bonded to one of the N-H sites of the pyridyl-hydrazone of another complex. One ligand is omitted for clarity and only its N binding sites are shown. Crystals were obtained by vapor diffusion of diisopropylether into a solution of **1-E** and $CaCl_2$ in methanol. CCDC 971153 contains the supplementary crystallographic data for this structure. (gray = carbon; green = chloride; blue= nitrogen, purple = calcium)

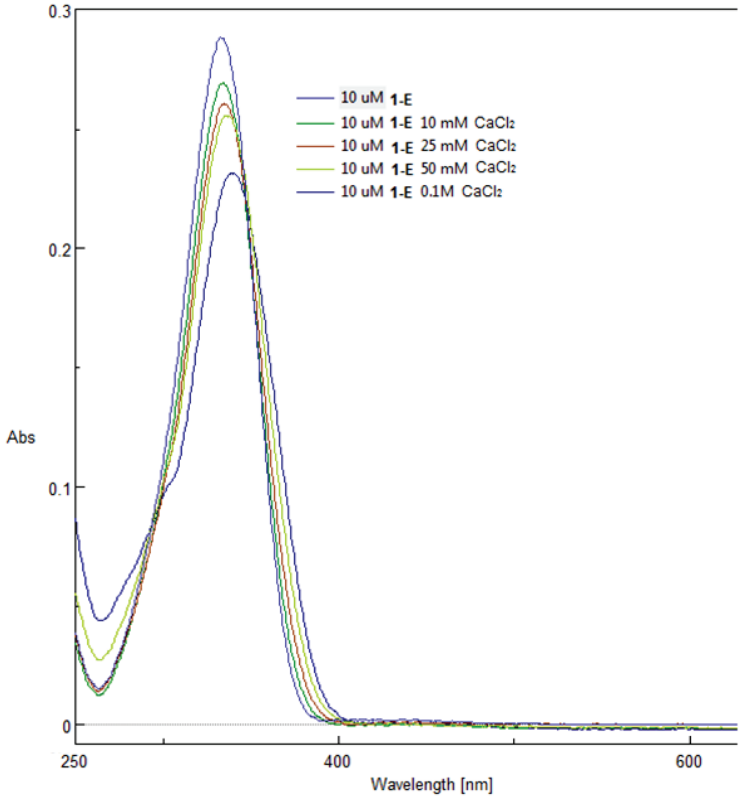

Fig. 2 UV/Vis spectra of **1-E** resulting from titration with incremental additions of $CaCl_2$ in 3:2 AN/W. These data were analyzed by the software Chem-Equili.[1] Stock solutions of ligand **1-E** were prepared in 3:2 AN/W (10 μM) and were titrating with $CaCl_2$. UV/Vis spectra were recorded after each addition.

The observed changes of the ligand absorption as a function of concentration of $CaCl_2$ were analyzed to give the association constant by the software ChemEquili.[2]

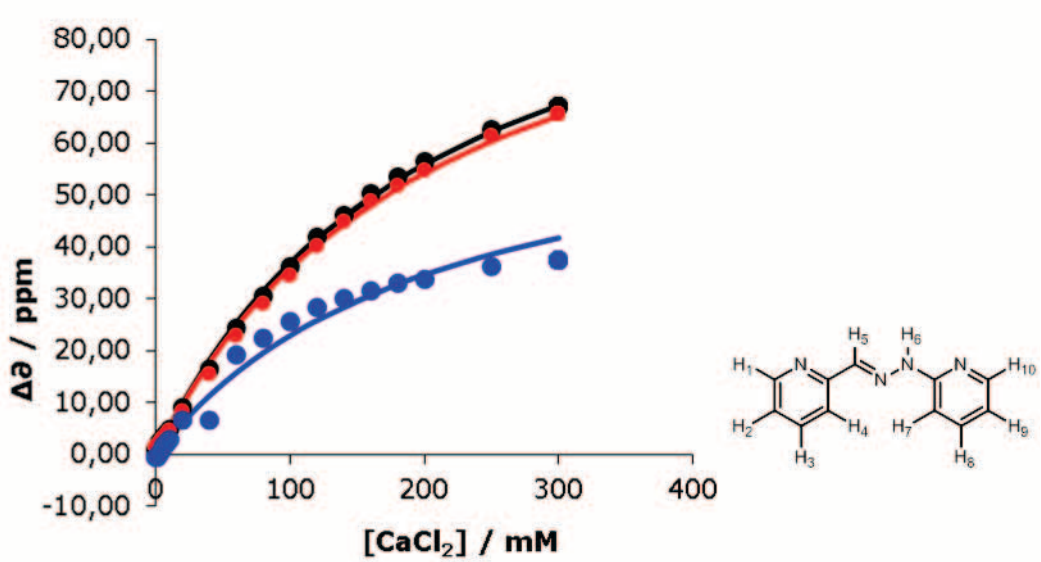

Fig. 3 Fitting for the experimental data of NMR shifts for three different protons (blue: H3, red: H10 and black: H1) of **1-E** upon addition of $CaCl_2$ in 3:2 AN/W at 25°C.

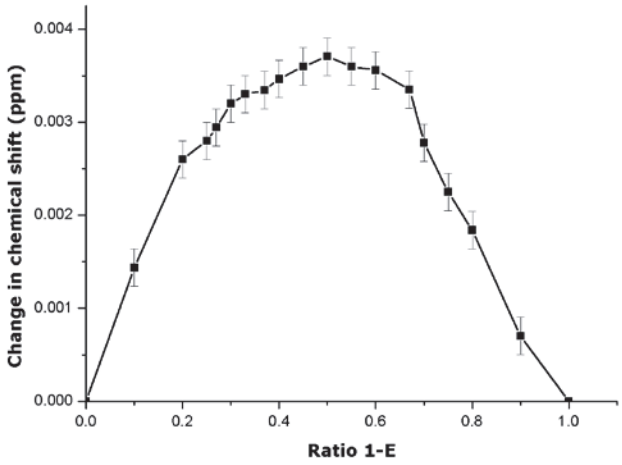

Fig. 4 Job plot of **1-E** with $CaCl_2$ showing the formation of a 1:1 complex in 10 mM 3:2 AN/W solution in agreement with the NMR observations. The lines just connect the experimental points for easier viewing.

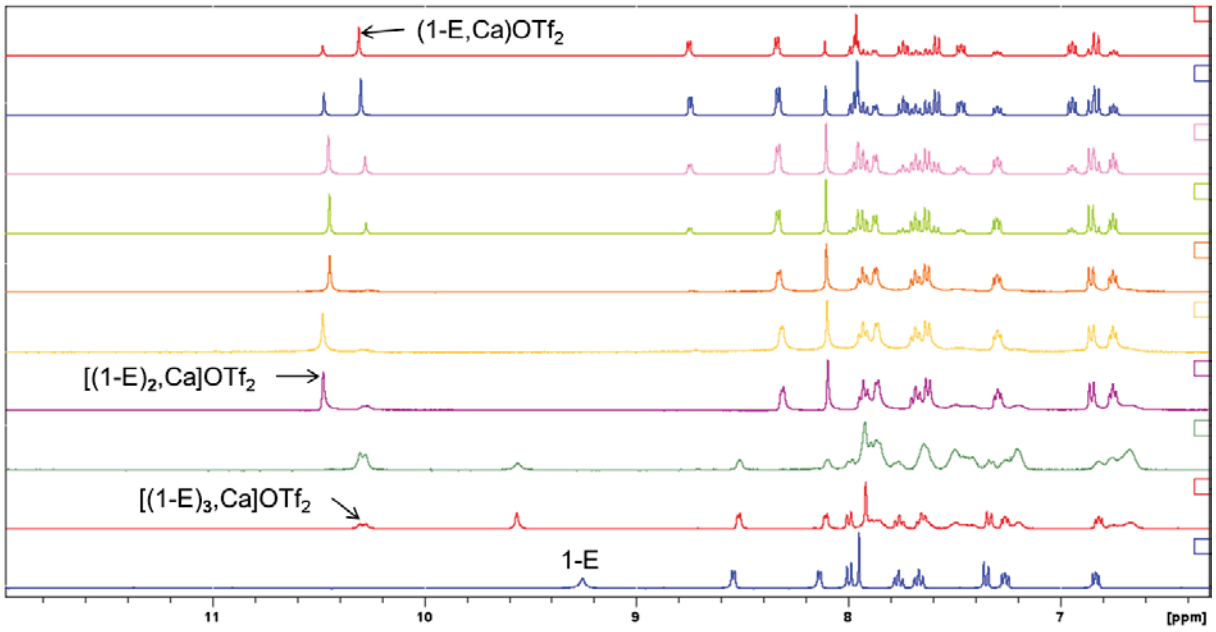

Fig. 5 A portion of the 400 MHz ^{1}H NMR spectra showing the evolution of the chemical shifts (ppm) of **1-E** upon addition of $Ca(OTf)_2$ in 10 mM AN-d_3 solution at -40°C (from bottom trace to top trace, 0, 0.15, 0.25, 0.43, 0.5, 0.6, 0.7, 0.8, 1, 1.5 eq. $Ca(OTf)_2$). The three complexes [(**1-E**)$_n$,**Ca**](**OTf**)$_2$ (n = 1, 2 and 3) are visible in slow exchange (the assignation of N*H* protons are indicated in the figure). The complex [(**1-E**)$_3$,**Ca**](**OTf**)$_2$ presents a doublet at 10.3 ppm due to the lack of symmetry of the complex (see X-ray structure in Figure 4 in the publication).

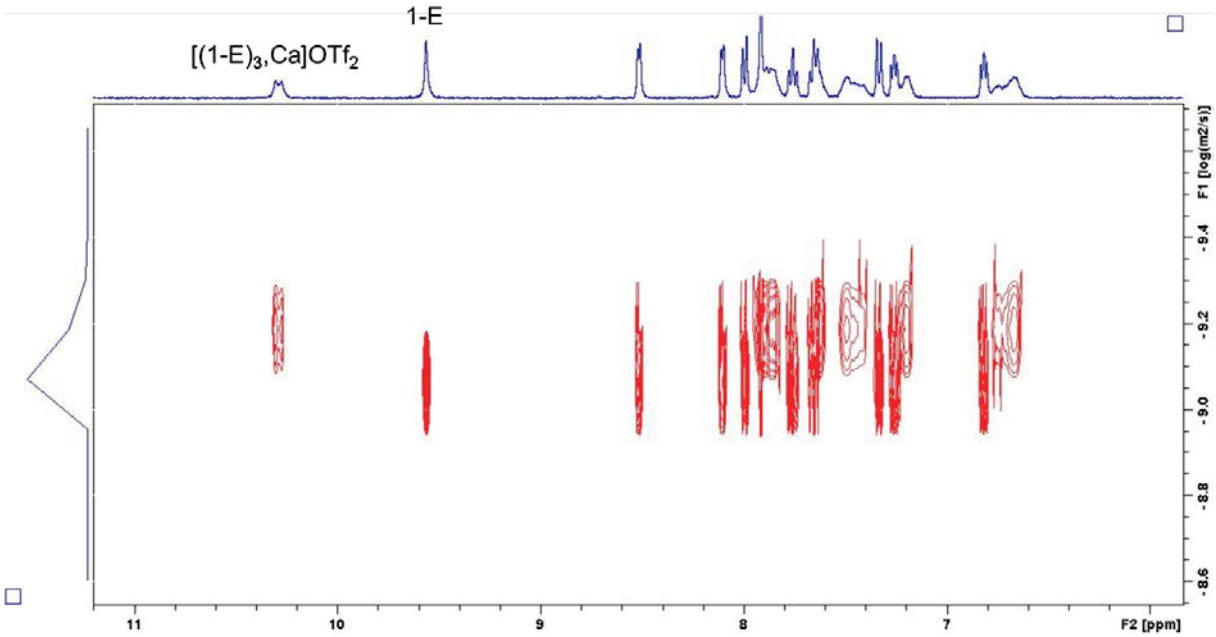

Fig. 6 DOSY NMR spectrum of **1-E** with 0.15 eq. $Ca(OTf)_2$ in 10 mM solution AN-d_3 at -40°C showing the two species **1-E** and [(**1-E**)$_3$,**Ca**](**OTf**)$_2$ and their different sizes.

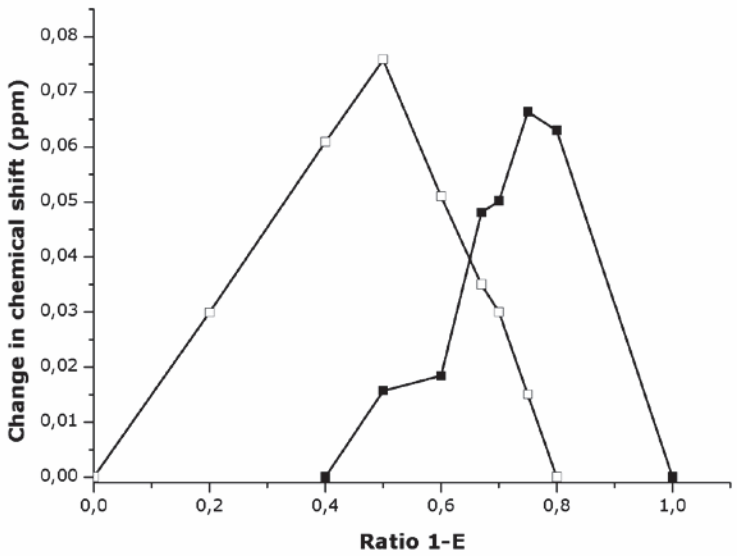

Fig. 7 Job plot of **1-E** with $Ca(OTf)_2$ showing the formation of 1:1 (□ trace) and 3:1 (■ trace) complexes on progressive addition of $Ca(OTf)_2$ in 10 mM AN solution at 25°C. The lines just connect the experimental points for easier viewing.

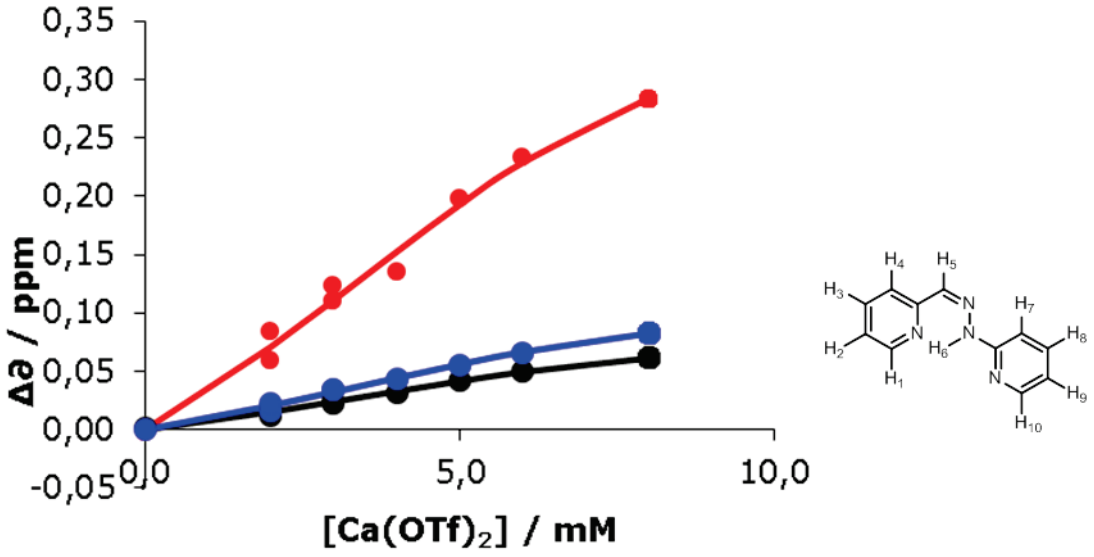

Fig. 8 Fitting for the experimental data of NMR shifts for two different protons (blue: H9, red: H5 and black: H1) of **1-Z** upon addition of $Ca(OTf)_2$ in AN at 25°C.

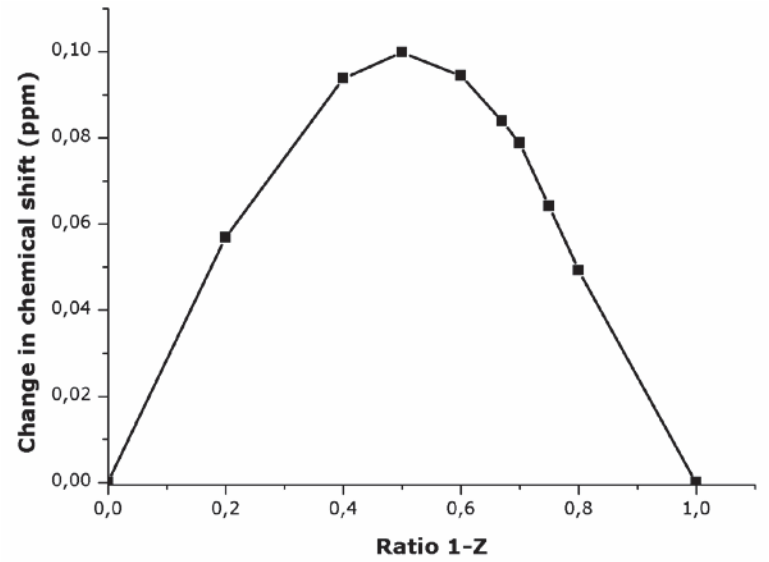

Fig. 9 Job plot of **1-Z** with $Ca(OTf)_2$ showing the formation of a 1:1 complex in 10 mM AN solution. The lines just connect the experimental points for easier viewing.

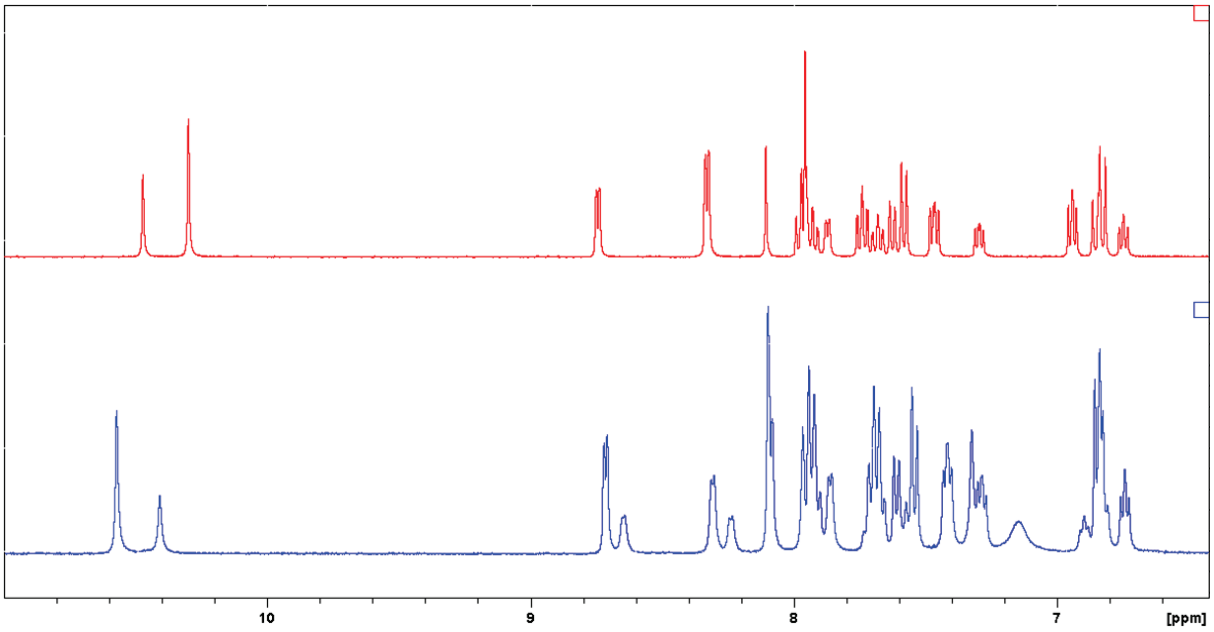

Fig. 10 A portion of the 400 MHz ^{1}H NMR competition spectrum (bottom trace) between $Ca(OTf)_2$, **1-E** and **1-Z** at -40°C (10 mM each) in AN-d_3 solution showing a change in the chemical signals ratio of N*H* (10.3-10.7 ppm) for the complexes of **1-E** compared to the spectrum (top trace) with $Ca(OTf)_2$ and **1-E** (10 mM each) in AN-d_3 solution.

Calcium binding by hydrazone 2-E.

The stability constant of the complex (**2-E,Ca**)$\mathbf{Cl_2}$ in 3:2 AN/W was found to be 5.4 ±1.1 M^{-1} at 25°C as determined by analysis of the UV-vis spectroscopy titration data obtained on progressive addition of $CaCl_2$ to **2-E** (see Fig. 11, SI). Nevertheless, in pure AN, no difference of bindings between **1-E** and **2-E** were noticed. A ^{1}H NMR competition experiment in pure AN did not shown preferential binding of calcium cations with **1-E** or **2-E**. The experiment showed the formation of the complexes [(**1-E**)$_2$,**Ca**]$\mathbf{Cl_2}$, [(**2-E**)$_2$,**Ca**]$\mathbf{Cl_2}$ and [(**1-E**),(**2-E**),**Ca**]$\mathbf{Cl_2}$ in almost the same quantity, proving that the complexes have the same stability in pure AN (see Fig. 12, SI). This experiment had been studied at -40°C to distinguish the different species in slow exchange.

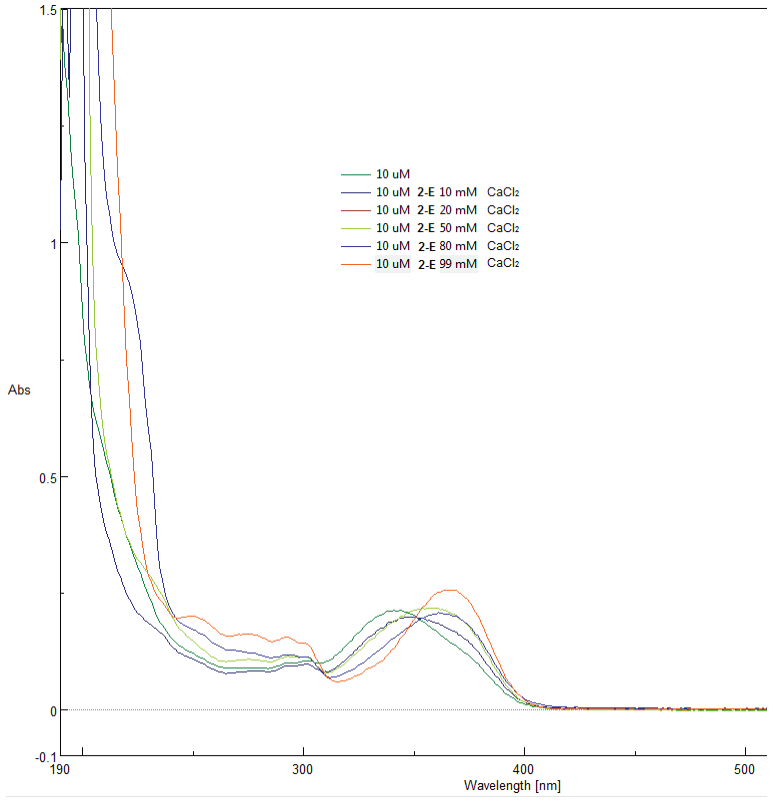

Fig. 11 UV/Vis spectra of **2-E** resulting from titration with incremental additions of $CaCl_2$ in 3:2 AN/W. These data were analyzed by the software Chem-Equili.[1]

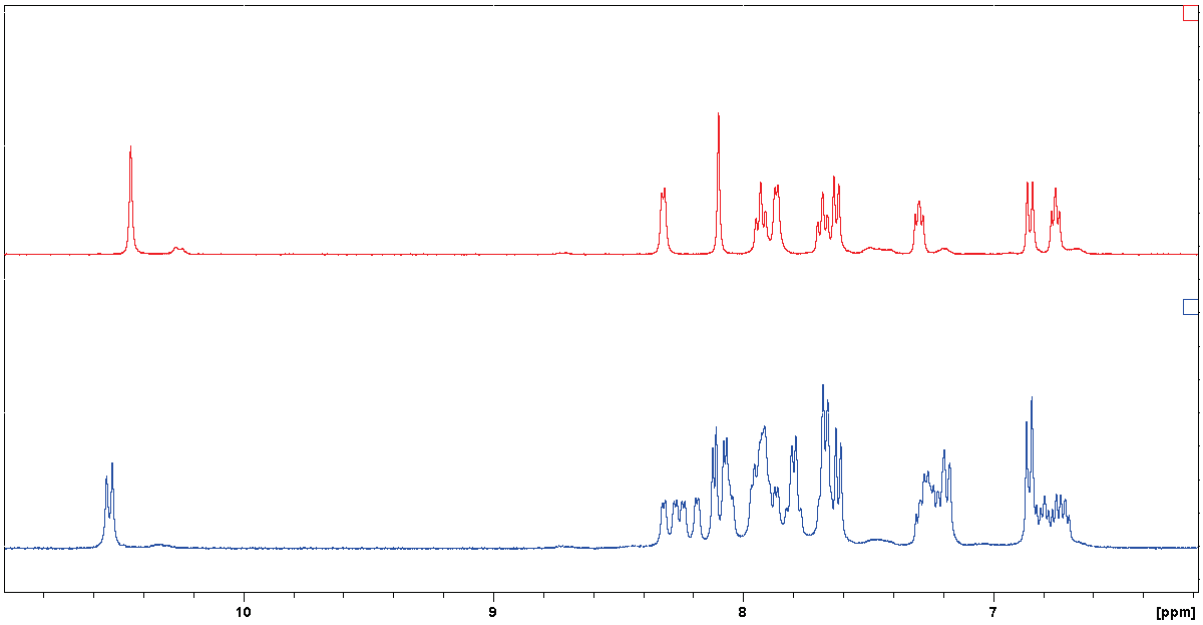

Fig. 12 A portion of the 400 MHz ^{1}H NMR competition spectrum (bottom trace) between $Ca(OTf)_2$, **1-E** and **2-E** (10 mM each) in AN-d_3 solution at -40°C showing two singulets at 10.5 ppm coming from a mixture of 2:1 complexes [(**1-E**)$_2$,**Ca**]**Cl**$_2$ and (**1-E**,**2-E**,**Ca**)**Cl**$_2$, compared to a portion of the 400 MHz ^{1}H NMR spectrum (top trace) of **1-E** with $Ca(OTf)_2$ (10 mM each) in AN-d_3 solution at -40°C showing the formation of the complex [(**1-E**)$_2$,**Ca**]**Cl**$_2$.

Strontium binding by hydrazone 1-E.

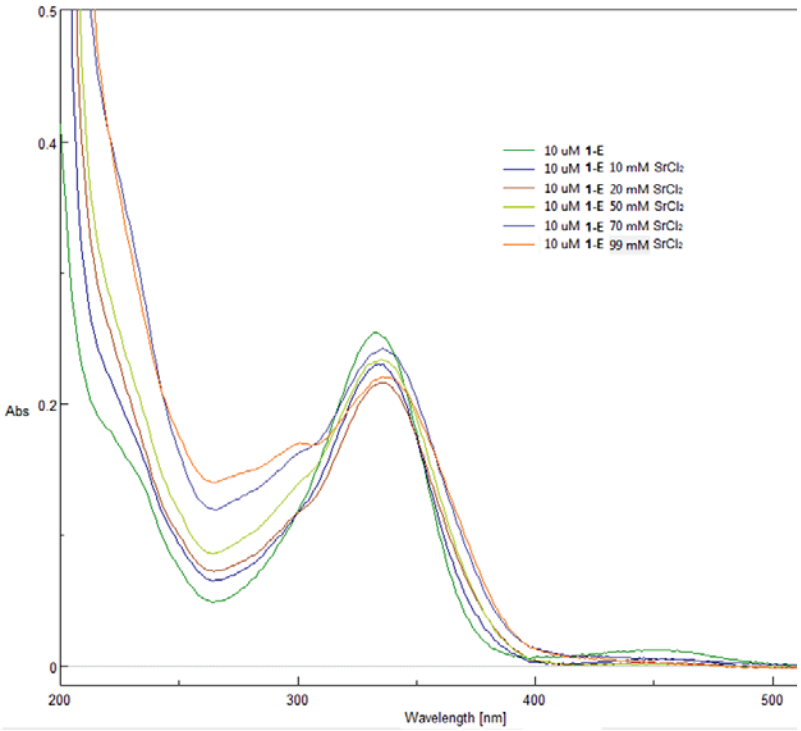

Fig. 13 UV/Vis spectra of **1-E** resulting from titration with incremental additions of $SrCl_2$ in 3:2 AN/W. These data were analyzed by the software Chem-Equili.[1]

This journal is © The Royal Society of Chemistry 2013

Calcium binding by acyl-hydrazone 3.

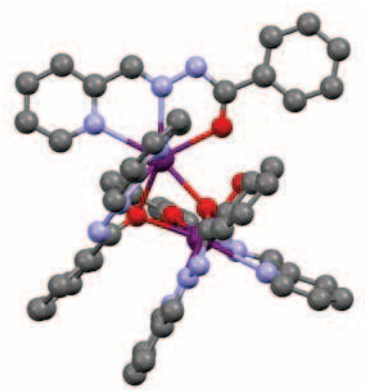

Fig. 14 Solid state molecular structure of the dimeric association of two neutral 2:1 **3-E**:Ca^{2+} complexes with the ligands in their ionized form at the N-H site. Crystals obtained by slow vapor diffusion of diisopropylether into a solution of **3-E** and $CaCl_2$ in AN. CCDC 971407 contains the supplementary crystallographic data for this structure. (gray = carbon; red = oxygen; blue= nitrogen, purple = calcium).

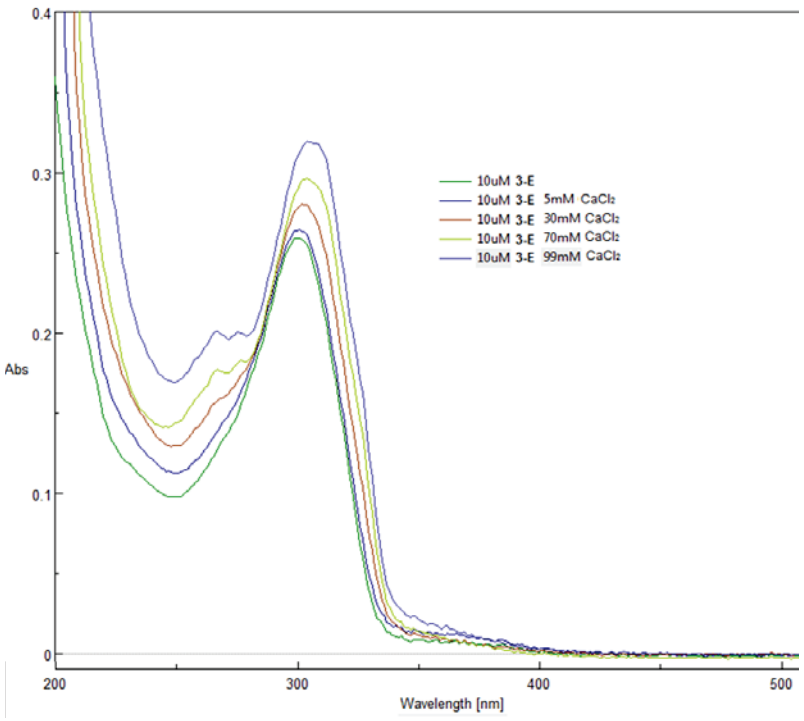

Fig. 15 UV/Vis spectra of **3-E** resulting from titration with incremental additions of $CaCl_2$ in 3:2 AN/W. These data were analyzed by the software Chem-Equili.[1]

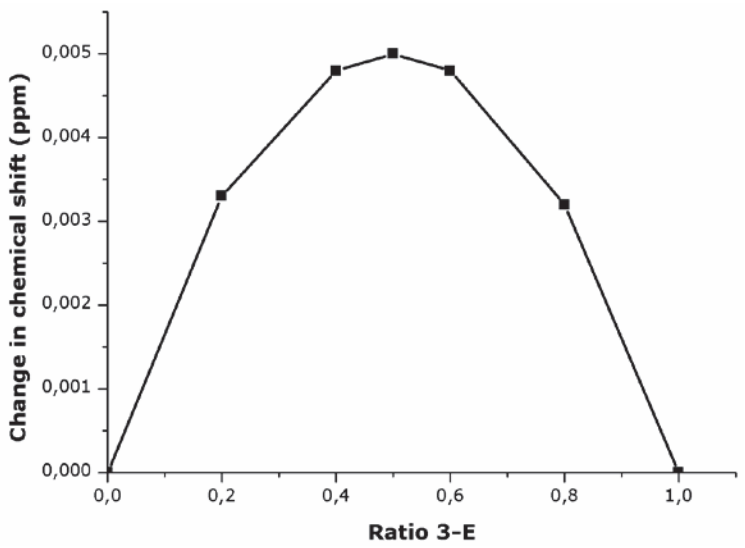

Fig. 16 Job plot of **3-E** with $CaCl_2$ showing the formation of a 1:1 complex in 10 mM 3:2 AN/W solution. The lines just connect the experimental points for easier viewing.

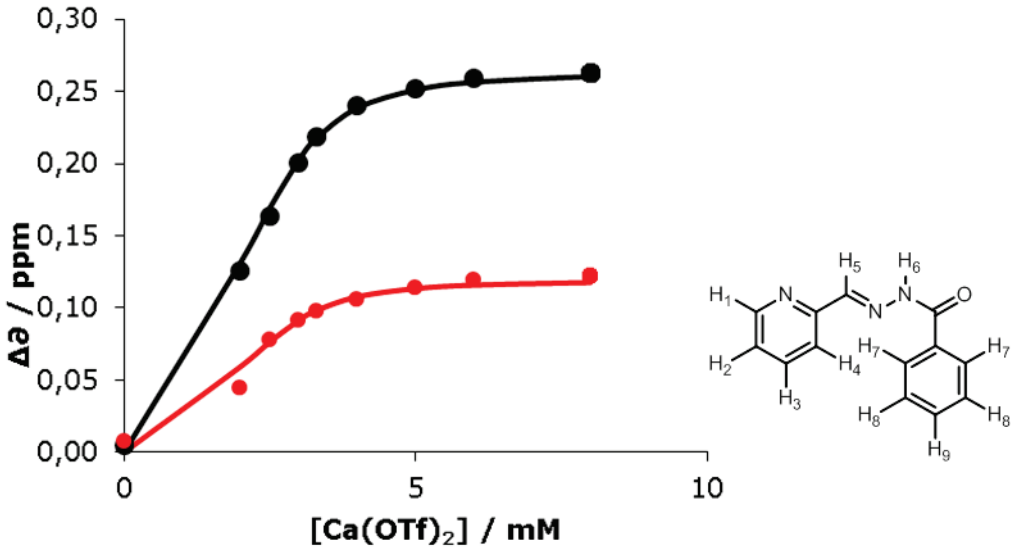

Fig. 17 Fitting for the experimental data of NMR shifts for two different protons (red: H1 and black: H3) of **3-E** upon addition of $Ca(OTf)_2$ in AN at 25°C.

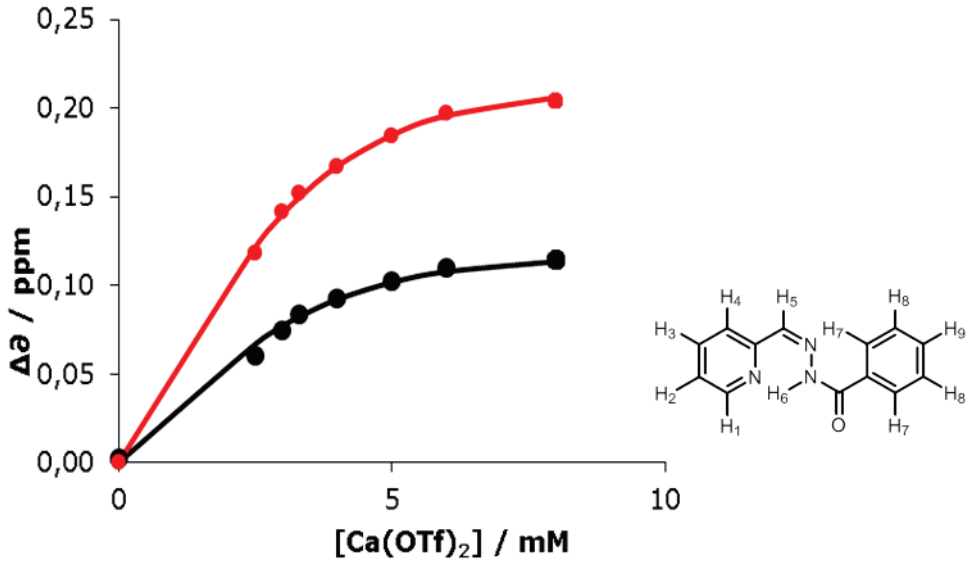

Fig. 18 Fitting for the experimental data of NMR shifts for two different protons (red: H3 and black: H5) of **3-Z** upon addition of $Ca(OTf)_2$ in AN at 25°C.

To confirm the preferential binding of Ca^{2+} with **3-E** compared to **3-Z**, a ^1H NMR competition experiment had been performed in pure AN 10 mM solution at 25°C in presence of $Ca(OTf)_2$, **3-E** and **3-Z** (10 mM each) and was compared to the ^1H NMR titration on progressive addition of $Ca(OTf)_2$ to **3-Z** (see Fig. 19, SI). The results showed that the signals of **3-Z** were found in the position where 0.3 eq. Ca^{2+} was bound to **3-Z**, so that 0.7 eq. Ca^{2+} was bound to **3-E** which confirmed the stronger binding of Ca^{2+} with **3-E**.

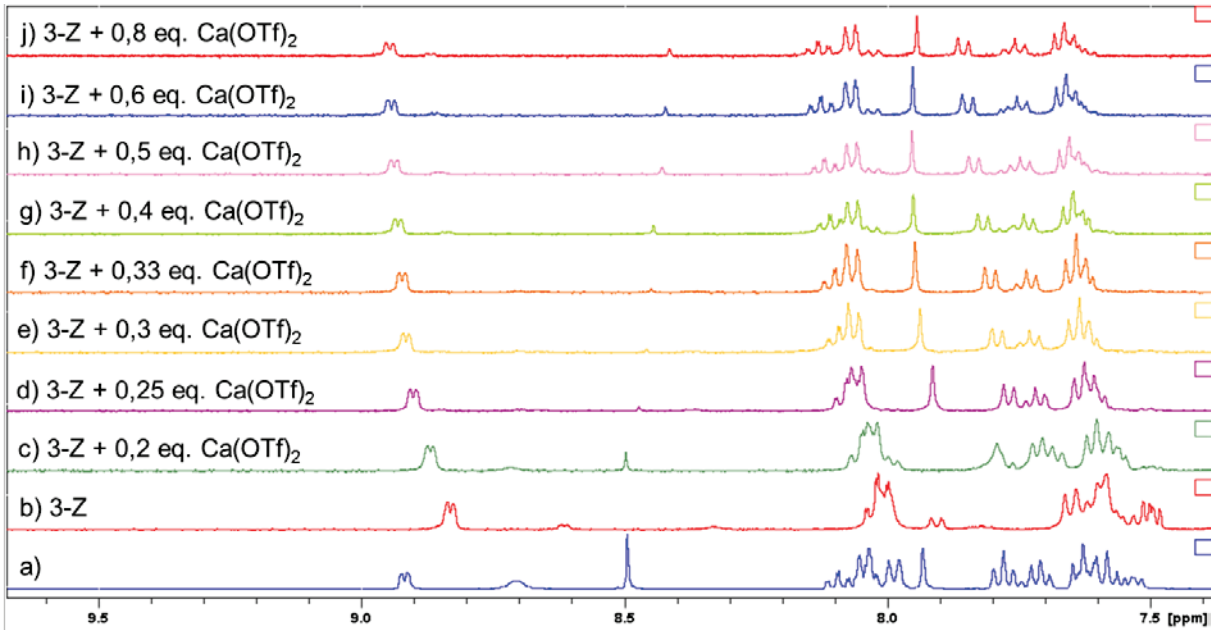

Fig. 19 A portion of the 400 MHz ^1H NMR competition spectra (a) between $Ca(OTf)_2$, **3-E** and **3-Z** (10 mM each) in AN-d_3 solution at 25°C compared to portions of the 400 MHz ^1H NMR spectra (b-j) of **3-Z** (10 mM) with progressive addition of $Ca(OTf)_2$ in AN-d_3 solution, showing a preferential binding of Ca^{2+} to **3-E** because the chemical shifts of **3-Z** in the competition experiment (a) superpose with the chemical shifts of the spectrum (e) with 0.3 eq. $Ca(OTf)_2$.

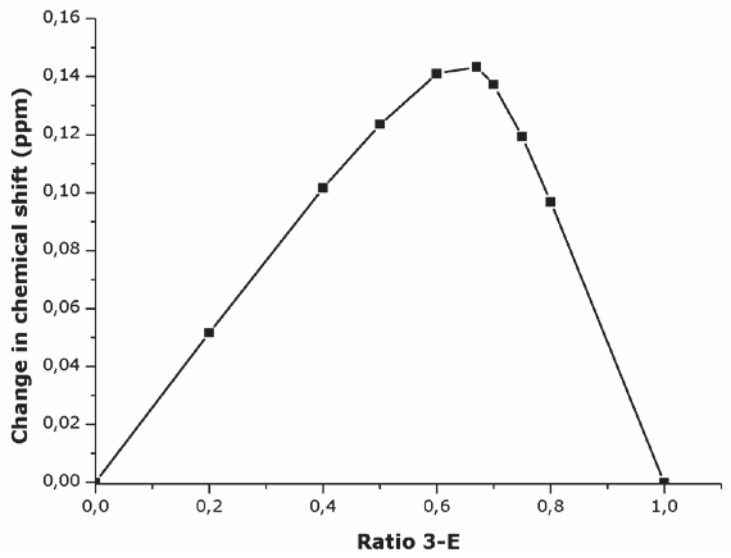

Fig. 20 Job plot of **3-E** with $Ca(OTf)_2$ showing the formation of a 2:1 complex in 10 mM AN solution. The lines just connect the experimental points for easier viewing.

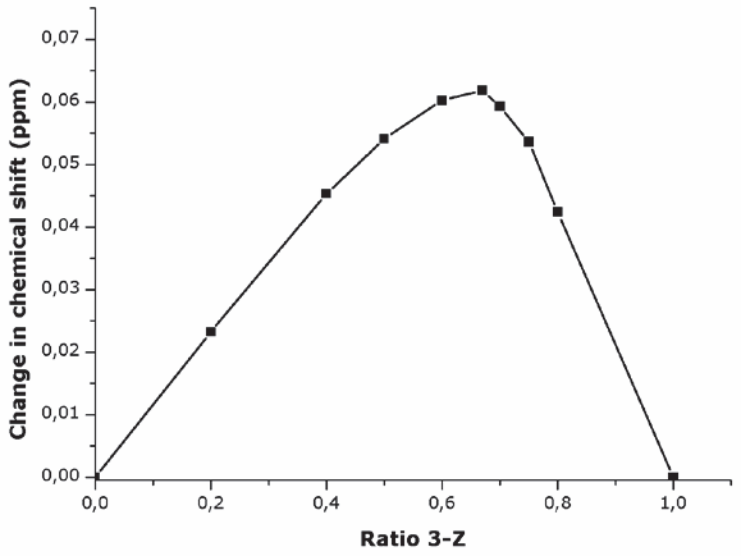

Fig. 21 Job plot of **3-Z** with $Ca(OTf)_2$ showing the formation of a 2:1 complex in 10 mM AN solution. The lines just connect the experimental points for easier viewing.

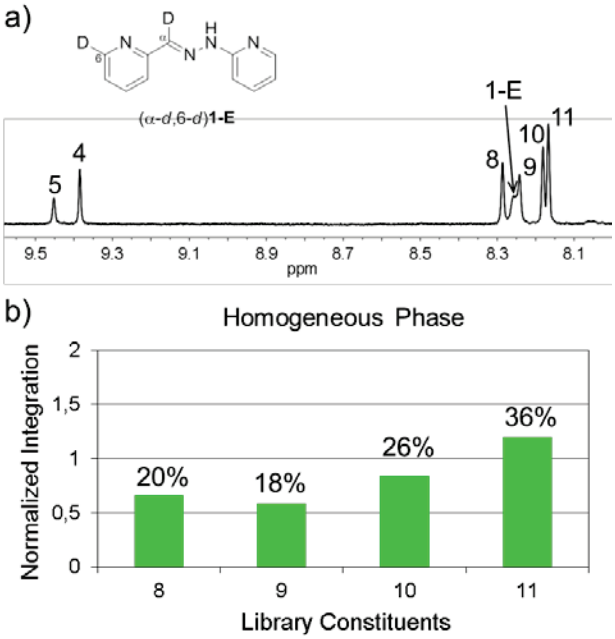

Fig. 22 Distribution of the dynamic covalent library of imines **8**-**11** (40 mM each) in a single phase of 3:2 AN/W in the presence of 306 mM $CaCl_2$. a) 400 MHz ^{1}H NMR spectrum of the mixture: –CH=N- proton signals of imines **8**-**11** in the 8.1-8.4 ppm region; -CHO proton signals of unreacted **4** and **5** between 9.3 and 9.5 ppm. The arrow indicates the remaining proton signal H_6 of partially deuterated **1-E**. b) Amounts and fractions of the four different imine constituents **8**-**11**, determined by integration of the corresponding –CH=N- proton signals against an external standard.

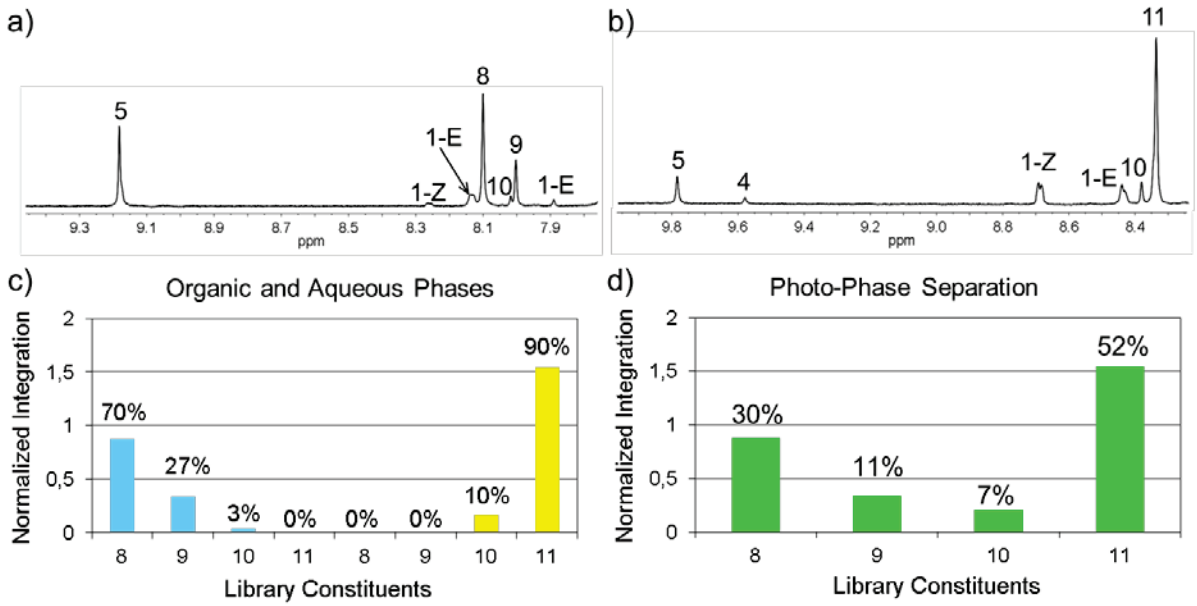

Fig. 23 Distribution of the dynamic covalent library of imines **8**-**11** (40 mM each), in the presence of 305 mM $CaCl_2$, upon phase separation of a 3:2 AN/W solution into a biphasic system by light irradiation for 9h. (Top) 400 MHz ^{1}H NMR spectrum of the aqueous (a) and organic phase (b); –CH=N- and -CHO proton signals in the 8.0-8.5 and 9.1-9.8 ppm region respectively. (c) Distributions of the four different imine constituents in the respective phases, aqueous (blue, left) and organic (yellow, right), determined by integration of the corresponding –CH=N proton signals against an external standard. (d) Integrated amounts and fractions of the four different imine constituents **8**-**11** summed over both phases.

This journal is © The Royal Society of Chemistry 2013

References:

(1) Pohjala, E.K. *Finn. Chem. Lett.* **1980**, *4*, 126-128.

(2) CHEM-EQUILI is a computer program for the calculation of equilibrium constants from many types of equilibrium data (IR, NMR, UV/Vis and fluorescence spectrophotometry, potentiometry, calorimetry, conductimetry…). It is possible to use any combination of such kinds of methods simultaneously for reliable calculations of equilibrium constants. For a detailed description see: Solov'ev, V. P.; Vnuk, E.; Strakhova, N. N.; Kazachenko, V. P.; Belsky, V. K.; Varnek, A. A.; Volkova, T. A.; Wipff, G. *J. Chem. Soc. Perkin Trans.* 2 **1998**, 1489.